Research Article

On Throughput-Fairness Tradeoff in Virtual MIMO Systems with Limited Feedback

Alexis A. Dowhuszko,[1] Graciela Corral-Briones,[1] Jyri Hämäläinen,[2] and Risto Wichman[3]

[1] *Digital Communications Research Laboratory, National University of Cordoba (UNC) - CONICET, Avenida Velez Sarsfield 1611, X5016GCA Cordoba, Argentina*
[2] *Department of Communications and Networking, Helsinki University of Technology (TKK), P.O. Box 3000, FIN-02015 TKK, Finland*
[3] *Department of Signal Processing and Acoustics, Helsinki University of Technology (TKK) - Smart and Novel Radios (SMARAD) Centre of Excellence, P.O. Box 3000, FIN-02015 TKK, Finland*

Correspondence should be addressed to Alexis A. Dowhuszko, adowhuszko@efn.unc.edu.ar

We investigate the performance of channel-aware scheduling algorithms designed for the downlink of a wireless communication system. Our study focuses on a two-transmit antenna cellular system, where the base station can only rely on quantized versions of channel state information to carry out scheduling decisions. The motivation is to study the interaction between throughput and fairness of practical spatial multiplexing schemes when implemented using existing physical layer signaling, such as the one that exists in current wideband code division multiple access downlink. Virtual MIMO system selects at each time instant a pair of users that report orthogonal (quantized) channels. Closed-form expressions for the achievable sum-rate of three different channel-aware scheduling rules are presented using an analytical framework that is derived in this work. Our analysis reveals that simple scheduling procedures allow to reap a large fraction (in the order of 80%) of the sum-rate performance that greedy scheduling provides. This overall throughput performance is obtained without affecting considerably the optimal short-term fairness behavior that the end users would perceive.

1. Introduction

The deployment of multiple *transmit* (Tx) antennas at the *base station* (BS) has emerged as an effective way for improving the overall throughput in a wireless communication system. This is because multiuser *multiple-input multiple-output* (MIMO) downlink systems offer multiple channel directions to send independent information streams to multiple users simultaneously within the same resource block, capitalizing the so-called spatial multiplexing gain [1]. However, resource allocation in multiuser MIMO systems is not a trivial task because users should be selected taking into account not only their spatial compatibility, but also their individual channel strengths [2]. The construction of optimal schedulers in terms of throughput makes imperative the investigation of the sum-rate upper bound that can be achieved in this situation. However, such a myopic approach is not enough for real-life wireless applications

if the scheduler does not share common channel resources fairly among all the participating users as well. Based on this, intensive research has been carried out in the past few years to study the interaction between these two conflicting goals and design fair channel-aware scheduling rules for delay-constrained data connections. In this context, this work provides an analytical framework for quantifying the throughput gain of different multiuser scheduling strategies in MIMO downlink channel with different types of partial *channel state information* (CSI) in the transmitter. The use of a well-known fairness performance metric, Jain's fairness index [3], is also suggested as a simple way to evaluate the short-term fairness that is traded off at the expense of additional throughput gain.

Recent theoretical results show that the optimal transmission scheme in an MIMO downlink channel is *dirty paper coding* (DPC) [4], but it faces serious implementation

issues in practical systems due to its high complexity, especially when the number of participating users is large. *Linear beamforming* (LBF) is a suboptimal strategy in which each user stream is multiplied independently by a beamforming weighting vector for transmission through multiple antennas. Despite its reduced complexity, LBF achieves a large portion of DPC capacity and exhibits the best tradeoff between complexity and performance [5]. In particular, a simpler strategy based on *zero-forcing beamforming* (ZFBF) has been shown to be optimal in terms of sum capacity in the limit of a large number of users [6]. All these capacity results rely on the assumption that perfect CSI is available at the transmitter. However, this condition is hard to satisfy in practical systems, particularly when *frequency-division duplex* (FDD) is implemented because in practice mobiles report their channel estimates to the BS via a rate-constrained reverse channel.

One of the simplest approaches to reduce feedback overhead involves each user quantizing his instantaneous vector channel according to a finite collection of vectors (beamformer codebook) that is maintained at both extremes of the link [7]. After selecting the optimal quantization vector, receiver feeds back the corresponding codeword index through a B-bit (per user) reverse channel at the beginning of each transmission block. This feedback is used to capture the *channel direction information* (CDI), and was first considered for point-to-point MIMO channels in [8, 9]. System sum-rate capacity with only CDI is bounded as the number of users increases because *channel quality information* (CQI) is not available in transmission to exploit multiuser diversity and obtain the double-logarithmic growth in system throughput with the number of users [10]. Based on this, both CDI and CQI feedbacks are necessary if we want to achieve both multiplexing and multiuser diversity gains at the same time. As expected, we later show that CQI should be the channel magnitude in low Tx power regime, while it should be proportional to the *signal-to-interference* power *ratio* (SIR) when Tx power is high.

Limited feedback techniques have already been considered in 3G cellular standards, where two antenna schemes have been emphasized so far due to implementation constraints. In *3G Partnership Project* (3GPP), *closed-loop* (CL) *transmit-diversity* (TD) techniques come in two classes: quantized phase information (mode 1) and direct channel quantization (mode 2) [11]. The quantized phase algorithm uses a fixed number of bits to quantize phase angles to perform equal gain beamforming at the transmitter. The direct channel quantization allocates a fixed number of bits for the gain and phase of each channel entry separately, as opposed to more sophisticated vector quantization techniques that quantize gain and phase jointly. Our motivation is to study the performance when combining channel-aware scheduling rules with ZFBF prefiltering in case of practical (commercial) beamformer codebook designs. Note that this principle is equivalent to virtual MIMO concept for the uplink of a *time-division multiple-access* (TDMA)-based cellular system, where many users with only one Tx antenna transmit independently to the BS on the same resource block. Our analysis reveals that in the presence of 3GPP physical

layer signaling, the additional multiuser diversity gain that is obtained at the cost of relegating fairness considerations over short time scales is quite important. However, it was also observed that the implementation of simpler scheduling procedures, such as the one presented in [12], offers a good balance between implementation complexity, short-term fairness, and system sum-rate performance. Although we concentrate on the two CL techniques in the FDD mode of the *wideband code division multiple access* (W-CDMA) downlink, a similar procedure can be used to extend the analysis to other FDD MIMO systems with limited feedback.

The rest of the paper is organized as follows: Section 2 introduces the system model, presents the feedback model for CDI and CQI, and describes the scheduling strategies and spatial prefiltering technique that will be analyzed. Section 3 studies the statistics of desired signal energy and mutual interference, proposes a probability distribution approximation for them, and derives an accurate closed-form expression for the achievable rate per user when BS simultaneously transmits to a pair of semiorthogonal users without exploiting multiuser diversity. Section 4 extends the analysis when channel norm CQI or SIR CQI is available in transmission to perform user selection. Section 5 introduces the criterion that is used to carry out the fairness study of the different schemes over short-time scales. Section 6 analyzes the performance of the different scheduling strategies, quantifying the different tradeoffs between throughput and fairness that they provide. Finally, conclusions are drawn in Section 7.

2. System Model

The system consists of a single BS with $M_t = 2$ Tx antennas and K active *user equipments* (UEs) with single-element antennas. In case of flat fading and rich scattering, the channel gain from a Tx antenna t to a UE k is described by a zero-mean circularly symmetric complex Gaussian *random variable* (RV) $h_{k,t}$, for $t = 1, \ldots, M_t$ and $k = 1, \ldots, K$. We assume that all UEs are homogeneous and experience independent fading, and that they have a low-rate, reliable, and delay-free feedback channel to the BS.

A block fading channel model is employed, that is, channels remain constant during each block of transmitted symbols, and channels between temporally separate transmission blocks are independent. Transmitted codewords of fixed rate span multiple independent fading blocks; therefore, when the number of blocks is large, the system is able to achieve nonzero ergodic capacity. Note that instead of fixed rate codes, *high-speed downlink packet access* (HSDPA) [13] exploits variable rate coding, where the BS selects modulation and coding scheme according to CQI reports. However, it has been shown in [14] that both fixed rate and variable rate coding strategies achieve the same capacity when channel variation satisfies a compatibility assumption meaning that the input distribution that maximizes mutual information is the same regardless of the channel state. We note that block fading channels with constant Tx power satisfy this compatibility assumption.

In our system model, the signal received by a user k is

$$r_k = \mathbf{h}_k \mathbf{x} + n_k, \quad k = 1, \ldots, K, \tag{1}$$

where $\mathbf{x} \in \mathbb{C}^{M_t \times 1}$ is the transmitted vector signal from the BS antennas containing information symbols of selected users, $\mathbf{h}_k \in \mathbb{C}^{1 \times M_t}$ is the channel gain vector, and n_k is zero-mean complex additive white Gaussian noise with power N_0. In order to facilitate the analysis, the channel and noise entries are normalized to have unit variance. The average power constraint of the input signal implies that $\mathbb{E}\{\mathbf{x}^\dagger \mathbf{x}\} \leq P$, where P is the total Tx energy per channel use, $(\cdot)^\dagger$ denotes Hermitian transpose, and $\mathbb{E}\{\cdot\}$ denotes expectation. As with HSDPA, we do not consider the possibility of employing fast power control mechanisms at the BS; thus, P remains fixed. Since the noise has unitary variance, P takes on the meaning of total Tx *signal-to-noise* power *ratio* (SNR).

As the number of participating users grows, the introduction of user selection mechanisms enables the BS to choose up to M_t out of K mobiles to use the channel. In this context, $\mathcal{S}$ is the set that contains the indices of selected UEs at any given time. Transmit vector $\mathbf{x}$ is related to information symbols $\{s_i : i \in \mathcal{S}\}$ via linear beamforming; that is, $\mathbf{x} = \sum_{i \in \mathcal{S}} \mathbf{w}_i s_i$, where Tx weights $\{\mathbf{w}_i : i \in \mathcal{S}\}$ are appropriately selected according to BS spatial prefiltering technique and quantized versions of channel states $\{\hat{\mathbf{h}}_i : i \in \mathcal{S}\}$ available in transmission. Based on this, rewriting (1) in a more convenient way, it is possible to observe that received signal

$$r_k = \underbrace{(\mathbf{h}_k \mathbf{w}_k) s_k}_{d_k: \text{Desired Signal}} + \underbrace{\sum_{l \in \mathcal{S}, l \neq k} (\mathbf{h}_k \mathbf{w}_l) s_l}_{q_k: \text{Mutual Interference}} + \underbrace{n_k}_{\text{Noise}}, \quad k \in \mathcal{S} \tag{2}$$

is actually composed by three different parts. Active user set $\mathcal{S}$ is chosen according to the implemented scheduling policy and will ideally try to provide a reasonable tradeoff between throughput and fairness according to quality-of-service requirements of the supported application.

2.1. Feedback Model for Channel Direction Information and Channel Quality Information.

The feedback scheme assumes that each UE has perfect CSI in reception, and each of them quantizes the normalized channel vector $\tilde{\mathbf{h}}_k = \mathbf{h}_k / \|\mathbf{h}_k\|$ to a unit norm M_t-dimensional vector $\hat{\mathbf{h}}_k$, which is selected from a common quantization codebook $\mathcal{C} = \{\mathbf{c}_1, \ldots, \mathbf{c}_{2^B}\}$, where B refers to the number of reported CDI bits per mobile user. Each UE quantizes its channel vector to the codeword that forms the minimum angle to it, or equivalently

$$\hat{\mathbf{h}}_k = \arg\max_{\mathbf{c}_i \in \mathcal{C}} \cos^2 \angle(\tilde{\mathbf{h}}_k, \mathbf{c}_i) = \arg\max_{\mathbf{c}_i \in \mathcal{C}} |\tilde{\mathbf{h}}_k \mathbf{c}_i^\dagger|^2. \tag{3}$$

Note that only the index i needs to be reported because quantization codebook $\mathcal{C}$ is known to both transmitter and mobile users a priori.

Narula et al. noticed in [7] that CL beamforming is invariant to the channel being multiplied by $e^{j\vartheta}$ for any phase angle ϑ. Therefore, it can be assumed that the first coefficient $\hat{h}_{k,1}$ of channel vector $\hat{\mathbf{h}}_k$ is real, and without loss of generality, CDI feedback solution can be fully characterized by $(M_t - 1)$ complex coefficients. More precisely, when focusing on 2 Tx antennas, CDI feedback is composed by a single complex coefficient $\hat{h}_{k,2} = \hat{\alpha}_k e^{-j\hat{\phi}_k}$, where $\hat{\alpha}_k$ and $\hat{\phi}_k$ are quantized magnitude and phase of the weight applied in the second Tx antenna. Specifically, in W-CDMA mode 1 CL TD solution, only phase information of the feedback weight is quantized with 2 bits (i.e., the magnitude remains constant), while in mode 2 both magnitude and phase are independently quantized with 1 bit and 3 bits, respectively [11]. In both cases, uniform quantization is applied for phase information. In mode 2, the stronger channel receives 6 dB more power than the weaker one. Even though CL TD mode 2 was later removed from the specification with the motivation of simplifying the 3GPP standard, we also consider this feedback mode in order to quantify performance gain when the amount of reported CDI grows.

In addition to the CDI, each user feeds back a CQI that is used at BS for scheduling purposes. In this work, we consider two different definitions for CQI:

$$Q(\mathbf{h}_k) = \|\mathbf{h}_k\|^2,$$

$$\breve{Q}(\mathbf{h}_k) = \frac{\mathbb{E}\{|d_k|^2\}}{\mathbb{E}\{|q_k|^2\}} \tag{4}$$

$$= \frac{|\mathbf{h}_k \mathbf{w}_k|^2}{\sum_{l \in \mathcal{S}, l \neq k} |\mathbf{h}_k \mathbf{w}_l|^2},$$

that are proportional to the selected users channel norm and SIR, respectively. Channel norm CQI is suitable for noise-limited communication systems, such as those that employ TDMA schemes or spatial multiplexing strategies with imperfect CSI at the transmitter in low-SNR regions. Note that this is the CQI definition that W-CDMA specification contains. On the other hand, SIR CQI does a better job in the presence of interference-limited systems, such as those that implement spatial multiplexing policies with imperfect CSI at the transmitter in high Tx power regimes. We assume that the CQI is reported to the BS without quantization; however, previous works have already observed that the number of bits for CQI quantization can be kept relatively low with an appropriate CQI feedback design [15, 16].

2.2. Scheduling Strategies.

Seeking a reasonable balance between throughput and fairness, a scheduler achieving *proportional fairness* (PF) criterion was first proposed in [17]. This PF scheduler selects at each time slot the user with the highest transmission rate relative to its current average throughput. In the classical version, the average rate is tracked by an exponential window with time constant t_c. The proper selection of parameter t_c allows to control the maximum starvation period (i.e., the maximum time between two successive service offerings) for the packet scheduling scheme. The combination of PF scheduler along with ZFBF precoding has been proposed in [6] as a natural alternative to provide an equal share of common resources

among users in a *space-division multiple-access* (SDMA) system with multiuser diversity. Even though important results on tradeoffs between throughput and fairness have been reported, no closed-form formula for sum-rate performance has been provided since PF algorithm is hard to analyze. Keeping this in mind, we will study the behavior of simpler schemes that will allow us to derive closed-form expressions for the performance of ZFBF-PF when t_c is tuned to maximize system throughput or fairness, respectively.

Optimal user set solution in terms of throughput demands an exhaustive search over all possible groups with up to M_t out of K members at a time, taking into account their spatial compatibility and CQI. In order to avoid this search in the presence of many users, suboptimal *semiorthogonal user selection* (SUS) procedure was used instead as an accurate approximation for ZFBF-PF upper bound, see [6, 10]. On the other hand, we use pure *orthogonal round-robin* (ORR) scheme proposed in [12] as a simple lower bound for ZFBF-PF when CSI is not taken into account to perform scheduling. We note that the idea behind pure ORR scheme is simple. Select both, primary and secondary users in round-robin (RR) taking into account their spatial compatibility. Since primary user is selected according to its waiting time at the BS, all active users will have an explicit guarantee to be scheduled at least one time in a round.

2.3. Zero-Forcing Beamforming Scheme.

Let $\hat{\mathbf{H}}(\mathcal{S}) = [\hat{\mathbf{h}}_{\pi(1)}^T, \ldots, \hat{\mathbf{h}}_{\pi(|\mathcal{S}|)}^T]^T$ be the concatenated unit norm quantized vectors of selected users in set $\mathcal{S} = \{\pi(1), \ldots, \pi(|\mathcal{S}|)\}$, where $(\cdot)^T$ denotes vector transpose. The ZFBF matrix is given by the pseudoinverse of the channel as

$$\mathbf{W}(\mathcal{S}) = \hat{\mathbf{H}}(\mathcal{S})^+ = \hat{\mathbf{H}}(\mathcal{S})^\dagger [\hat{\mathbf{H}}(\mathcal{S})\hat{\mathbf{H}}(\mathcal{S})^\dagger]^{-1}, \quad (5)$$

where Tx weight $\mathbf{w}_{\pi(i)} \in \mathbb{C}^{M_t \times 1}$, obtained by normalizing the ith column of $\mathbf{W}$, represents Tx weight for user $\pi(i)$. In ZFBF, Tx weights satisfy orthogonality criterion in transmission; that is, $\hat{\mathbf{h}}_j \mathbf{w}_i = 0$ for $i, j \in \mathcal{S}$, $j \neq i$. Even though ZFBF is not the optimal choice among all possible LBF schemes, we focus on it because its analytical simplicity enables to obtain closed-form expressions for achievable sum-rate that are asymptotically optimal as the Tx power grows. Note that when the number of users K is large and the codebook contains orthogonal codewords (such as W-CDMA CL modes), $\mathbf{W}(\mathcal{S}) = \hat{\mathbf{H}}(\mathcal{S})^\dagger$.

3. Achievable Rate per Beam without Exploiting Multiuser Diversity

This section derives a closed-form expression for the achievable rate per user (beam) when BS simultaneously transmits to a pair of spatial-compatible UEs (i.e., semiorthogonal in terms of their quantized CDI) without considering CQI reports to perform scheduling. The derived expression is used in Section 6 to quantify the actual system throughput of pure ORR and hybrid ORR proposals as well.

3.1. Probability Distributions of Desired Signal and Mutual Interference.

Following the model (2) we construct two RVs,

$$X_k = |\mathbf{h}_k \mathbf{w}_k|^2, \qquad Y_k = |\mathbf{h}_k \mathbf{w}_l|^2. \quad (6)$$

Here, the first RV gives the desired signal energy while the second RV represents the contribution of mutual interference due to simultaneous transmission. In these equations, $\mathbf{w}_k = \hat{\mathbf{h}}_k^\dagger$ is the Tx weight vector that maximizes received energy for user k (i.e., the best Tx weight), while $\mathbf{w}_l = \hat{\mathbf{h}}_l^\dagger$ is the Tx weight vector that minimizes received energy of the same user (i.e., worst Tx weight). In the coming sections, we deduce usable formulae for achievable rates in different cases based on modeling the distributions of X_k and Y_k, denoted by $f_x(x)$ and $f_y(y)$, by chi-square (χ^2) distribution approximations. To justify this claim, we use Nakagami's distribution [18]

$$f(\gamma) = \frac{1}{\Gamma(\mathcal{F})} \left(\frac{\mathcal{F}}{\mathcal{G}}\right)^{\mathcal{F}} \gamma^{\mathcal{F}-1} e^{-(\mathcal{F}/\mathcal{G})\gamma} \quad (7)$$

as an accurate approximation to model the signal energy behavior of our RVs, where $\Gamma(\cdot)$ denotes the Gamma function and

$$\mathcal{G} = \mathbb{E}\{\gamma\}, \qquad \mathcal{F} = \frac{\mathcal{G}^2}{\mathbb{E}\{(\gamma - \mathcal{G})^2\}} \quad (8)$$

represent the so-called SNR gain and fading figure, respectively. Note that the SNR gain provides information on the coherent combining gain, whereas the fading figure indicates the degree of signal variation. If $\mathcal{F} \in \mathbb{N}$, then $f(\gamma)$ is the normalized χ^2-distribution with $r = 2\mathcal{F}$ degrees of freedom. If we select Tx weights randomly, then there is neither coherent combining power gain (i.e., $\mathcal{G} = 1$), nor Tx diversity gain (i.e., $\mathcal{F} = 1$). On the other hand, in the presence of unquantized Tx weights, full Tx beamforming gain is achieved (i.e., $\mathcal{G} = 2$ and $\mathcal{F} = 2$).

According to the analysis presented in Appendix A.2, the first-order corrected version when approximating $f_x(x)$ by an χ^2-distribution with 4 degrees of freedom is given by

$$f_x(x) \approx \left(\frac{2}{\mathcal{G}_x}\right)^2 x e^{-(2/\mathcal{G}_x)x}(b_2 x^2 + b_1 x + b_0),$$
$$b_0 = 2\left(\frac{\mathbb{E}\{X_k^2\}}{\mathcal{G}_x^2} - 1\right), \quad b_1 = \frac{2(1-b_0)}{\mathcal{G}_x}, \quad b_2 = -\frac{2(1-b_0)}{(3\mathcal{G}_x^2)}. \quad (9)$$

Similarly, Appendix A.1 derives the first-order corrected version when $f_y(y)$ is approximated by an exponential distribution (i.e., χ^2-distribution with 2 degrees of freedom). In this case,

$$f_y(y) \approx \left(\frac{1}{\mathcal{G}_y}\right) e^{-(1/\mathcal{G}_y)y}(a_2 y^2 + a_1 y + a_0),$$
$$a_0 = \frac{\mathbb{E}\{Y_k^2\}}{(2\mathcal{G}_y^2)}, \quad a_1 = \frac{2(1-a_0)}{\mathcal{G}_y}, \quad a_2 = -\frac{(1-a_0)}{(2\mathcal{G}_y^2)}. \quad (10)$$

3.2. Probability Distribution Approximations with Deterministic Codebook Design. Let us assume that CDI codebook is selected using a deterministic design with fixed number of bits to quantize the gain and phase portions of each channel independently, see Section 2.1. Then, each weight vector admits an orthogonal counterpart. Hence, for any weight $\mathbf{w}_k$, there exists a weight $\mathbf{w}_l$ such that $\mathbf{w}_k^\dagger \mathbf{w}_l = 0$. Note that while beams are orthogonal in transmission, the orthogonality is lost in the receiver because Tx weights are selected based on quantized versions of actual channel direction $\widetilde{\mathbf{h}}_k$. After working out (6), we arrive at

$$
\begin{aligned}
X_k &= |w_{1,k}|^2 |h_{k,1}|^2 + |w_{2,k}|^2 |h_{k,2}|^2 \\
&\quad + 2|w_{1,k}||w_{2,k}||h_{k,1}||h_{k,2}|\cos\varphi_k, \\
Y_k &= |w_{2,k}|^2 |h_{k,1}|^2 + |w_{1,k}|^2 |h_{k,2}|^2 \\
&\quad - 2|w_{1,k}||w_{2,k}||h_{k,1}||h_{k,2}|\cos\varphi_k,
\end{aligned}
\tag{11}
$$

where $\varphi_k = \angle(h_{k,1}) - \angle(h_{k,2}) + \hat{\phi}_k$ is the phase difference between both channel gains after applying the corresponding Tx weight vector. Let us denote by Z_k the sum of X_k and Y_k. Then, we find by (11) that

$$
Z_k = X_k + Y_k = |h_{k,1}|^2 + |h_{k,2}|^2
\tag{12}
$$

follows an χ^2-distribution with 4 degrees of freedom and mean $\mathbb{E}\{Z_k\} = 2$.

The SNR gains and fading figures for both W-CDMA CL TD modes are derived analytically in Appendix B, see Table 1. According to these results, fading figures $\mathcal{F}_x \approx 2$ and $\mathcal{F}_y \approx 1$ in the both CL TD methods. This indicates that the shapes of distributions $f_x(x)$ and $f_y(y)$ are close to χ^2-distribution with $r_x = 4$ and $r_y = 2$ degrees of freedom, respectively. (A similar procedure can be used to compute both SNR gains and fading figures when the BS is equipped with more than two Tx antennas, with the only difference that mutual interference would become the sum of $(M_t - 1)$ i.i.d. RVs in this situation.) It has already been observed in [12] that these approximations greatly simplify the computation of closed-form expressions for achievable sum-rate. However, in order to have a better distribution fitting, we propose to use the first-order correction for χ^2-distribution approximation, as detailed in Appendix A. Coefficients a_i and b_i for both CL TD feedback modes have been derived analytically based on the first two raw moments of RVs X_k and Y_k. These moments are computed in Appendix B, and coefficients are presented in Table 2.

3.3. Achievable Rate for Spatial Multiplexing with CDI and No CQI. When BS applies SDMA to simultaneously serve a pair of UEs that report orthogonal CDI codewords (no CQI), the achievable rate per user when Tx power is evenly divided between both users (i.e., $P/2$) is

$$
C_k(P) = \mathbb{E}\left\{\log_2\left(1 + \frac{(1/2)PX_k}{(1/2)PY_k + N_0}\right)\right\}
\tag{13}
$$

$$
= \log_2(e)\left[\mathbb{E}\{\log_e(Z_k + N_0')\} - \mathbb{E}\{\log_e(Y_k + N_0')\}\right],
\tag{14}
$$

TABLE 1: SNR gains and fading figures in case of CL TD mode 1 and 2.

(a) SNR gains

	Mode 1	Mode 2
$\mathcal{G}_x$	$1 + \sqrt{\dfrac{1}{2}}$	$1.3 + 1.6\sin\dfrac{\pi}{8}$
$\mathcal{G}_y$	$1 - \sqrt{\dfrac{1}{2}}$	$0.7 - 1.6\sin\dfrac{\pi}{8}$

(b) Fading figures

	Mode 1	Mode 2
$\mathcal{F}_x$	1.9104	1.9919
$\mathcal{F}_y$	0.7714	0.6816

TABLE 2: Coefficients for first-order correction χ^2-approximation with CL TD mode 1 and 2.

(a) $f_x(x)$ approximation

	Mode 1	Mode 2
b_0	1.0469	1.0041
b_1	−0.0549	−0.0043
b_2	0.0107	0.0007

(b) $f_y(y)$ approximation

	Mode 1	Mode 2
a_0	1.1481	1.2336
a_1	−1.0116	−5.3265
a_2	0.8634	15.1827

where $N_0' = 2N_0/P$. Based on the fact that Z_k is χ^2 distributed with 4 degrees of freedom ($\mathcal{G}_z = 2$),

$$
\mathbb{E}\{\log_e(Z_k + N_0')\} = \int_0^\infty \log_e(z + N_0') z e^{-z}\, dz.
\tag{15}
$$

At this stage, we use the relation derived in Appendix C

$$
\int_0^\infty \log_e(\gamma + c)\beta(\beta\gamma)^n e^{-\beta\gamma}\, d\gamma = n!\left[\log_e(c) + e^{\beta c}\sum_{i=0}^n E_{i+1}(\beta c)\right],
\tag{16}
$$

where $E_n(z)$ represents the exponential integral function of order n, see (5.1.4) of [19]. After combining (15) and (16), we obtain

$$
\mathbb{E}\{\log_e(Z_k + N_0')\} = \log_e(N_0') + e^{N_0'}\left[E_1(N_0') + E_2(N_0')\right].
\tag{17}
$$

To compute the latter expectation in (14), we use approximation (10) and formula (16), that is,

$$
\mathbb{E}\{\log_e(Y_k + N'_0)\}
$$

$$
\approx \int_0^\infty \log_e(y + N'_0)\left(\frac{1}{\mathcal{G}_y}\right)e^{-(1/\mathcal{G}_y)y}\left(a_2 y^2 + a_1 y + a_0\right)dy
$$

$$
= \left(2a_2\mathcal{G}_y^2 + a_1\mathcal{G}_y + a_0\right)\left[\log_e(N'_0) + e^{N'_0/\mathcal{G}_y}E_1\left(\frac{N'_0}{\mathcal{G}_y}\right)\right]
$$

$$
+ \left(2a_2\mathcal{G}_y^2 + a_1\mathcal{G}_y\right)e^{N'_0/\mathcal{G}_y}E_2\left(\frac{N'_0}{\mathcal{G}_y}\right) + \left(2a_2\mathcal{G}_y^2\right)e^{N'_0/\mathcal{G}_y}E_3\left(\frac{N'_0}{\mathcal{G}_y}\right),
$$

$$(18)$$

where coefficients a_i and SNR gain $\mathcal{G}_y$ depend on the number of bits assigned to report CDI to the transmitter (see Tables 2 and 1). Replacing (17) and (18) in (14), final approximation to estimate the achievable rate per beam with only CDI feedback is obtained.

3.3.1. Low-SNR Regime. Assume that Tx power is small. Then, after applying Taylor series expansion in (13), we find that

$$
C_k(P) \approx \log_2(e)\frac{1}{2}\frac{P}{N_0}\mathbb{E}\{X_k\}, \quad P \ll N_0. \tag{19}
$$

Hence, achievable rate of an individual user decays linearly with Tx power in a low-SNR regime.

3.3.2. High-SNR Regime. As expected, proposed SDMA scheme admits an interference-limited behavior in high Tx power regime since reported CDI is not perfect. A formula for this upper bound is obtained from expression of $C_k(P)$, given by (14) combined with (17) and (18), as follows. First, we write all exponential integral functions of order $n > 1$ in terms of $E_1(z)$ using recursive relationship (5.1.14) of [19], that is,

$$
E_{n+1}(z) = \frac{1}{n}\left[e^{-z} - zE_n(z)\right], \quad n = 1, 2, \ldots. \tag{20}
$$

Then, we let P grow and apply approximation for $E_1(z)$ that is valid for small z values, that is,

$$
E_1(z) \approx -\epsilon_0 - \log_e(z) \quad z \longrightarrow 0. \tag{21}
$$

Here, $\epsilon_0 = 0.5772\ldots$ is Eulers' constant. After these preparations, we find that all terms containing logarithm of P vanish, and we are able to compute the final limit when $P \to \infty$. It turns out that asymptotic formula admits expression in terms of SNR gain and fading figure as

$$
\lim_{P \to \infty} C_k(P) \approx \log_2(e)\left[\frac{3\mathcal{F}_y + 1}{4\mathcal{F}_y} - \log_e(\mathcal{G}_y)\right]. \tag{22}
$$

According to this formula, asymptotic upper bounds are equal to 3.3211 and 5.1223 bps/Hz for CL TD modes 1 and 2, respectively.

3.4. Achievable Rate for Single User Transmission with CDI and No CQI. For comparison purposes, we also introduce a single user approach (or TDMA scheme), where all Tx power is assigned to a single user in RR fashion. In this situation, achievable rate becomes

$$
C^{\text{TDMA}}(P) = \mathbb{E}\left\{\log_2\left(1 + \frac{PX_k}{N_0}\right)\right\}
$$

$$
= \log_2(e)\left[\mathbb{E}\left\{\log_e\left(X_k + \frac{N_0}{P}\right)\right\} - \log_e\left(\frac{N_0}{P}\right)\right]. \tag{23}
$$

Here, we could use first-order corrected distribution $f_x(x)$ according to (9), but from Table 2 we find that $b_0 \approx 1$ and $b_1, b_2 \approx 0$ for both CL TD feedback modes. Hence,

$$
\mathbb{E}\left\{\log_e\left(X_k + \frac{N_0}{P}\right)\right\} \approx \int_0^\infty \log_e\left(x + \frac{N_0}{P}\right)\left(\frac{2}{\mathcal{G}_x}\right)^2 xe^{-(2/\mathcal{G}_x)x}\,dx \tag{24}
$$

and we can apply relation (16) to derive the final closed-form expression

$$
C^{\text{TDMA}}(P) \approx \log_2(e)e^{(2N_0)/(P\mathcal{G}_x)}\left[E_1\left(\frac{2N_0}{P\mathcal{G}_x}\right) + E_2\left(\frac{2N_0}{P\mathcal{G}_x}\right)\right], \tag{25}
$$

where SNR gain $\mathcal{G}_x$ depends on the number of bits used for CDI quantization, see Table 1.

3.4.1. Low-SNR Regime. Applying Taylor series expansion in (23), we arrive to an approximation that resembles the one presented in (19). Based on this, it is possible to conclude that achievable rate admit linear dependence on Tx power when SNR is low.

3.4.2. High-SNR Regime. Rewriting $E_2(\cdot)$ in (25) using recursive formula (20) and considering approximation (21), we see that

$$
C^{\text{TDMA}}(P) \approx \log_2(e)\left[1 - \epsilon_0 - \log_e\left(\frac{2N_0}{P\mathcal{G}_x}\right)\right]
$$

$$
\approx \log_2\left(\frac{P}{N_0}\right) + \log_2(\mathcal{G}_x), \quad P \gg N_0. \tag{26}
$$

Thus, achievable rate increases logarithmically with the Tx power when SNR is high. As expected, the use of CL TD provides an additional logarithmic SNR gain in this case.

4. Achievable Rate per Beam When Exploiting Multiuser Diversity

When the number of active users is large, there exist with high probability more than one user reporting any given CDI codeword. In this situation, the best strategy in terms of throughput is to select the UE with the best CQI among

all users with identical CDI. In this section, we extend the previous analysis to a scenario where the BS exploits users CQI to reap multiuser diversity gain. Derived expressions are used in Section 6 to quantify the actual system throughput of ZFBF-SUS and hybrid ORR proposals as well.

4.1. Alternative RVs to Study the Effect of CQI Feedback. According to the model introduced in Section 2.1, each UE feeds back a quantized version of its CDI selected from a common codebook. Thus, we construct the following two RVs:

$$\tilde{X}_k = |\tilde{\mathbf{h}}_k \mathbf{w}_k|^2 = \frac{1}{\|\mathbf{h}_k\|^2} |\mathbf{h}_k \mathbf{w}_k|^2 = \frac{X_k}{Z_k},$$
$$\tilde{Y}_k = |\tilde{\mathbf{h}}_k \mathbf{w}_l|^2 = \frac{1}{\|\mathbf{h}_k\|^2} |\mathbf{h}_k \mathbf{w}_l|^2 = \frac{Y_k}{Z_k}. \tag{27}$$

In our model both, channel direction $\tilde{\mathbf{h}}_k$ and channel magnitude $\|\mathbf{h}_k\|$ are independent. Therefore, Tx weight vector $\mathbf{w}_k$ (and $\mathbf{w}_l$) does not depend on the channel strength. Thus, it is possible to conclude that both $\tilde{X}_k$ and $\tilde{Y}_k$ are independent with respect to Z_k. This property will be useful when deriving performance behavior for the different SDMA schedulers that will be analyzed.

4.2. Achievable Rate for Spatial Multiplexing with CDI and Channel Norm CQI. In this part, we analyze the effect of exploiting multiuser diversity when CQI reports are proportional to the channel norm (i.e., $Q(\mathbf{h}_k) = \|\mathbf{h}_k\|^2 = Z_k$). The procedure consists of selecting the user with the largest channel norm among all the users that report a given CDI codeword. The analysis that we apply here is similar to the one already employed in Section 3.3. However, the main difference is found in the modeling of the desired signal and mutual interference, that become $Z_{(n)} \tilde{X}_k$ and $Z_{(n)} \tilde{Y}_k$, respectively, with $Z_{(n)} = \max_{i=1,\dots,n} Z_i$. Based on these considerations, the achievable rate per beam when there are n users reporting the same CDI codeword is

$$C_{(n)}^{\text{Norm}}(P) = \mathbb{E}\left\{ \log_2 \left(1 + \frac{(1/2)PZ_{(n)}\tilde{X}_k}{(1/2)PZ_{(n)}\tilde{Y}_k + N_0} \right) \right\} \tag{28}$$
$$= \log_2(e)[\mathbb{E}\{\log_e(Z_{(n)} + N_0')\} - \mathbb{E}\{\log_e(Z_{(n)}\tilde{Y}_k + N_0')\}], \tag{29}$$

where $Z_{(n)}$ is the largest order statistic of n *independent* and *identically distributed* (i.i.d.) χ^2 RVs with 4 degrees of freedom ($g_z = 2$). Based on this, the *probability distribution function* (PDF) of $Z_{(n)}$ becomes

$$f_{z_{(n)}}(z) = \frac{\partial}{\partial z}[F_{z_{(n)}}(z)] = n[F_{z_{(n-1)}}(z)]f_z(z), \tag{30}$$

where $F_{z_{(n)}}(z)$ is the corresponding highest *cumulative distribution function* (CDF) given by

$$F_{z_{(n)}}(z) = \sum_{k=0}^{n} (-1)^k \binom{n}{k} e^{-zk}(1+z)^k. \tag{31}$$

At this stage, combining PDF expression (30) along with relation (16), we are now able to compute

$$\mathbb{E}\{\log_e(Z_{(n)} + N_0')\} = \int_0^\infty \log_e(z + N_0') f_{z_{(n)}}(z) dz$$
$$= \sum_{k=1}^{n} (-1)^{k+1} \binom{n}{k} \sum_{l=1}^{k} L_{k,l}(N_0'),$$
$$L_{k,l}(N_0') = \left[\frac{(k-1)!}{(k-l)!} \frac{l}{k^l} \right]$$
$$\times \left\{ \left[\sum_{m=1}^{l+1} E_m(kN_0')e^{kN_0'} \right] + \log_e(N_0') \right\}. \tag{32}$$

We now compute the approximation for the distribution of the resulting mutual interference $Z_{(n)}\tilde{Y}_k$. Firstly, based on the fact that RVs Z_k and $\tilde{Y}_k$ are independent, we have that

$$\mathbb{E}\{Z_{(n)}\tilde{Y}_k\} = \frac{g_y}{g_z}\mathbb{E}\{Z_{(n)}\} = \frac{g_y}{2}\mathbb{E}\{Z_{(n)}\},$$
$$\mathbb{E}\{Z_{(n)}^2 \tilde{Y}_k^2\} = \frac{\mathbb{E}\{Y_k^2\}}{\mathbb{E}\{Z_k^2\}}\mathbb{E}\{Z_{(n)}^2\} = \frac{\mathbb{E}\{Y_k^2\}}{6}\mathbb{E}\{Z_{(n)}^2\}, \tag{33}$$

where the statistics of Y_k are computed in Appendix B and first two raw moments of RV $Z_{(n)}$ can be derived analytically based on the PDF information presented in (30) (see [20]):

$$\mathbb{E}\{Z_{(n)}\} = \sum_{k=1}^{n} \left[(-1)^{k+1} \binom{n}{k} \sum_{l=1}^{k} \binom{k}{l} \frac{l(l+1)!}{k^{l+2}} \right],$$
$$\mathbb{E}\{Z_{(n)}^2\} = \sum_{k=1}^{n} \left[(-1)^{k+1} \binom{n}{k} \sum_{l=1}^{k} \binom{k}{l} \frac{l(l+2)!}{k^{l+3}} \right]. \tag{34}$$

When dealing with numbers of users that can be handled in realistic scenarios, it is possible to observe that $\mathcal{F}_{z_{(n)}\tilde{y}} \approx 1$. However, in order to show that this fading figure does not grow indefinitely with n, the following asymptotic upper bound for $\mathcal{F}_{z_{(n)}\tilde{y}}$ is derived:

$$\lim_{n \to \infty} \mathcal{F}_{z_{(n)}\tilde{y}} = \lim_{n \to \infty} \frac{\mathbb{E}^2\{Z_{(n)}\tilde{Y}_k\}}{\mathbb{E}\{Z_{(n)}^2 \tilde{Y}_k^2\} - \mathbb{E}^2\{Z_{(n)}\tilde{Y}_k\}}$$
$$= \frac{3g_y^2}{2\mathbb{E}\{Y_k^2\} - 3g_y^2}, \tag{35}$$

based on the fact that $\mathbb{E}^2\{Z_{(n)}\}/\text{Var}\{Z_{(n)}\} \to 0$ as n grows. We note that according to this formula, asymptotic upper bounds for this fading figure are equal to 1.8838 and 1.5509 for CL TD modes 1 and 2, respectively.

At this stage, we use (10) to approximate $f_{z_{(n)}\widetilde{y}}(u)$ in order to compute

$$
\mathbb{E}\{\log_e(Z_{(n)}\widetilde{Y}_k + N_0')\}
$$

$$
\approx \int_0^\infty \log_e(u + N_0')\left(\frac{1}{\mathcal{G}_{z_{(n)}\widetilde{y}}}\right)e^{-(1/\mathcal{G}_{z_{(n)}\widetilde{y}})u}
$$

$$
\times [a_2^{(n)}u^2 + a_1^{(n)}u + a_0^{(n)}]du
$$

$$
\approx [2a_2^{(n)}\mathcal{G}_{z_{(n)}\widetilde{y}}^2 + a_1^{(n)}\mathcal{G}_{z_{(n)}\widetilde{y}} + a_0^{(n)}]
$$

$$
\times \left[\log_e(N_0') + e^{N_0'/\mathcal{G}_{z_{(n)}\widetilde{y}}}E_1\left(\frac{N_0'}{\mathcal{G}_{z_{(n)}\widetilde{y}}}\right)\right] \tag{36}
$$

$$
+ [2a_2^{(n)}\mathcal{G}_{z_{(n)}\widetilde{y}}^2 + a_1^{(n)}\mathcal{G}_{z_{(n)}\widetilde{y}}]e^{N_0'/\mathcal{G}_{z_{(n)}\widetilde{y}}}E_2\left(\frac{N_0'}{\mathcal{G}_{z_{(n)}\widetilde{y}}}\right)
$$

$$
+ 2a_2^{(n)}\mathcal{G}_{z_{(n)}\widetilde{y}}^2 e^{N_0'/\mathcal{G}_{z_{(n)}\widetilde{y}}}E_3\left(\frac{N_0'}{\mathcal{G}_{z_{(n)}\widetilde{y}}}\right),
$$

where $\mathcal{G}_{z_{(n)}\widetilde{y}} = \mathbb{E}\{Z_{(n)}\widetilde{Y}_k\}$ and coefficients $a_i^{(n)}$ are derived analytically based on the first two raw moments of RV $Z_{(n)}\widetilde{Y}_k$ according to

$$
a_2^{(n)} = \frac{2\mathbb{E}\{Y_k^2\}\mathbb{E}\{Z_{(n)}^2\} - 6\mathcal{G}_y^2\mathbb{E}^2\{Z_{(n)}\}}{3\mathcal{G}_y^4\mathbb{E}^4\{Z_{(n)}\}},
$$

$$
a_1^{(n)} = \frac{-4\mathbb{E}\{Y_k^2\}\mathbb{E}\{Z_{(n)}^2\} + 12\mathcal{G}_y^2\mathbb{E}^2\{Z_{(n)}\}}{3\mathcal{G}_y^3\mathbb{E}^3\{Z_{(n)}\}}, \tag{37}
$$

$$
a_0^{(n)} = \frac{1}{3}\frac{\mathbb{E}\{Y_k^2\}\mathbb{E}\{Z_{(n)}^2\}}{\mathcal{G}_y^2\mathbb{E}^2\{Z_{(n)}\}}.
$$

Replacing (32), (36), and (37) in (29), the final closed-form approximation to estimate the achievable rate per beam with CDI and channel norm CQI feedback is obtained.

4.2.1. Low-SNR Regime.

Applying Taylor series expansion in (28) when the Tx power is low,

$$
C_{(n)}^{\text{Norm}}(P) \approx \log_2(e)\frac{1}{2}\frac{P}{N_0}\mathbb{E}\{Z_{(n)}\}\mathbb{E}\{\widetilde{X}_k\}
$$

$$
= \frac{\mathbb{E}\{Z_{(n)}\}}{\mathbb{E}\{Z_k\}}C_k(P) \quad P \ll N_0. \tag{38}
$$

The asymptotic behavior of the largest order statistic of n i.i.d. χ^2 RVs with $2M_t$ degrees of freedom has been reported in [15] to be

$$
\mathbb{E}\{\gamma_{(n)}\} \doteq \log_e(n) + \log_e\left[\frac{n^{M_t-1}}{(M_t-1)!}\right] + \epsilon_0, \tag{39}
$$

where notation $c_n \doteq d_n$ denotes asymptotic equivalence, defined as $\lim_{n\to\infty}(c_n/d_n) = 1$. Based on this, multiuser diversity gain in case of channel norm CQI and $M_t = 2$ is given by

$$
\frac{C_{(n)}^{\text{Norm}}}{C_k} \approx \frac{\mathbb{E}\{Z_{(n)}\}}{\mathbb{E}\{Z_k\}} \doteq \log_e(n) + \frac{1}{2}\epsilon_0 \quad P \ll N_0. \tag{40}
$$

4.2.2. High-SNR Regime.

A scheduler that relies on channel norm CQI to perform user selection has always the same asymptotic behavior, which does not depend on the number of active users. This is because SIR feedback is not considered for scheduling purposes; therefore, both the desired signal and mutual interference tend to grow with the same proportion as Tx power increases. So, we conclude that the upper bound for any smart scheduling scheme in this situation is identical to the one already obtained in Section 3.3.

4.3. Achievable Rate for Spatial Multiplexing with CDI and SIR CQI.

The effect of exploiting multiuser diversity when users reports are proportional to the received SIR is analyzed in this part. The procedure consists of scheduling the user with the largest SIR CQI

$$
\breve{Q}(\mathbf{h}_k) = \frac{X_k}{Y_k} = \frac{Z_k - Y_k}{Y_k} = \frac{Z_k(1 - \widetilde{Y}_k)}{Z_k\widetilde{Y}_k} = \frac{1 - \widetilde{Y}_k}{\widetilde{Y}_k}, \tag{41}
$$

which reduces to select the user that minimize $\widetilde{Y}_k$. Based on this, the achievable rate per beam when there are n users reporting the same CDI codeword and SIR CQI is given by

$$
C_{(n)}^{\text{SIR}}(P) = \mathbb{E}\left\{\log_2\left(1 + \frac{(1/2)PZ_k[1 - \widetilde{Y}_{(1)}]}{(1/2)PZ_k\widetilde{Y}_{(1)} + N_0}\right)\right\}
$$

$$
= \log_2(e)[\mathbb{E}\{\log_e(Z_k + N_0')\}
$$

$$
- \mathbb{E}\{\log_e(Z_k\widetilde{Y}_{(1)} + N_0')\}], \tag{42}
$$

where $\widetilde{Y}_{(1)} = \min_{i=1,\ldots,n}\widetilde{Y}_i$. We now need to find out an approximation for the distribution of the mutual interference $Z_k\widetilde{Y}_{(1)}$. Thus, we first study the behavior of RV $\widetilde{Y}_{(1)}$.

According to [9, 21], the CDF $F_{\widetilde{y}}(y)$ for any well-designed codebook satisfies $F_{\widetilde{y}^\star}(y) \geq F_{\widetilde{y}}(y)$ for $0 \leq y \leq 1$, where

$$
F_{\widetilde{y}^\star}(y) = \begin{cases} 2^B y^{M_t-1}, & 0 \leq y < 2^{-B/(M_t-1)}, \\ 1, & y \geq 2^{-B/(M_t-1)} \end{cases} \tag{43}
$$

represents quantization error CDF when *quantization cell upper bound* (QUB) approach is employed as a performance upper bound for any CDI codebook design. Based on this, it is possible to observe that the CDF of RV $\widetilde{Y}_k = 1 - |\widetilde{\mathbf{h}}_k\mathbf{w}_k|^2$ in case of $M_t = 2$ (and both CL TD feedback modes) will be upper bounded (in all its range) by the CDF of a uniform RV in $[0, 2^{-B}]$. Since the kth-order statistic of n uniformly distributed RVs in $[0, 1]$ is Beta distributed according to

$$
f_{u_{(k)}}(u) = \frac{n!}{(k-1)!(n-k)!}u^{k-1}(1-u)^{n-k}, \quad 0 \leq u \leq 1, \tag{44}
$$

the following expressions for the first two-ordered raw moments result:

$$
\mathbb{E}\{U_{(k)}\} = \frac{k}{n+1},
$$

$$
\mathbb{E}\{U_{(k)}^2\} = \frac{k(k+1)}{(n+1)(n+2)}. \tag{45}
$$

Taking into account that RVs Z_k and $\widetilde{Y}_k$ are independent, it is possible to lower bound the first two raw moments of mutual interference $Z_k \widetilde{Y}_{(1)}$ as

$$
\mathbb{E}\{Z_k \widetilde{Y}_{(1)}\} = \mathcal{G}_z \mathbb{E}\{\widetilde{Y}_{(1)}\} \gtrapprox 2\left(\frac{1}{2^B}\right)\left[\frac{1}{(n+1)}\right],
$$
$$
\mathbb{E}\{Z_k^2 \widetilde{Y}_{(1)}^2\} \gtrapprox 6\left(\frac{1}{4^B}\right)\left[\frac{2}{(n+1)(n+2)}\right],
\tag{46}
$$

where these approximations are asymptotically tight as n grows. According to these results, we see that fading figure $\mathcal{F}_{z\tilde{y}_{(1)}} \approx (n+2)/(2n+1)$, which is still close to 1 for both CL TD feedback modes when dealing with numbers of users that can be handled in realistic scenarios.

Using first-order corrected version presented in (10) to approximate $f_{z\tilde{y}_{(1)}}(u)$ by an exponential distribution with parameter $\mathcal{G}_{z\tilde{y}_{(1)}} = \mathbb{E}\{Z_k \widetilde{Y}_{(1)}\}$, it is possible to see that

$$
\begin{aligned}
&\mathbb{E}\{\log_e(Z_k \widetilde{Y}_{(1)} + N_0')\} \\
&\approx \int_0^\infty \log_e(u + N_0')\left(\frac{1}{\mathcal{G}_{z\tilde{y}_{(1)}}}\right)e^{-(1/\mathcal{G}_{z\tilde{y}_{(1)}})u} \\
&\qquad \times [\breve{a}_2^{(n)}u^2 + \breve{a}_1^{(n)}u + \breve{a}_0^{(n)}]du \\
&\approx \left[2\breve{a}_2^{(n)}\mathcal{G}_{z\tilde{y}_{(1)}}^2 + \breve{a}_1^{(n)}\mathcal{G}_{z\tilde{y}_{(1)}} + \breve{a}_0^{(n)}\right] \\
&\qquad \times \left[\log_e(N_0') + e^{N_0'/\mathcal{G}_{z\tilde{y}_{(1)}}}E_1\left(\frac{N_0'}{\mathcal{G}_{z\tilde{y}_{(1)}}}\right)\right] \\
&\quad + \left[2\breve{a}_2^{(n)}\mathcal{G}_{z\tilde{y}_{(1)}}^2 + \breve{a}_1^{(n)}\mathcal{G}_{z\tilde{y}_{(1)}}\right]e^{N_0'/\mathcal{G}_{z\tilde{y}_{(1)}}}E_2\left(\frac{N_0'}{\mathcal{G}_{z\tilde{y}_{(1)}}}\right) \\
&\quad + 2\breve{a}_2^{(n)}\mathcal{G}_{z\tilde{y}_{(1)}}^2 e^{N_0'/\mathcal{G}_{z\tilde{y}_{(1)}}}E_3\left(\frac{N_0'}{\mathcal{G}_{z\tilde{y}_{(1)}}}\right),
\end{aligned}
\tag{47}
$$

where coefficients $\breve{a}_i^{(n)}$ are derived analytically based on the first two raw moments of RV $Z_k \widetilde{Y}_{(1)}$:

$$
\breve{a}_2^{(n)} = (4^{B-2})\frac{(n-1)(n+1)^2}{(n+2)},
$$
$$
\breve{a}_1^{(n)} = -(2^{B-1})\frac{(n-1)(n+1)}{(n+2)},
\tag{48}
$$
$$
\breve{a}_0^{(n)} = \left(\frac{3}{2}\right)\frac{(n+1)}{(n+2)}.
$$

Replacing (17), (47), and (48) in (42), final closed-form approximation to estimate the achievable rate per beam with CDI and SIR CQI feedback is obtained.

4.3.1. Low-SNR Regime. Schedulers that rely on SIR CQI to perform user selection do not provide any multiuser diversity gain when Tx power is low. This is because they do not consider channel norm information to carry out decisions.

4.3.2. High-SNR Regime. Because the reported SIR CQI is not perfect, the achievable rate still has an interference-limited behavior in this situation. However, the corresponding asymptotic upper bound grows logarithmically with the number of users. The closed-form expression for this upper bound is obtained replacing SNR gain and fading figure approximations in (22). After some manipulations, final expression

$$
\lim_{P \to \infty} C_{(n)}^{\text{SIR}}(P) \approx \log_2(e)\left(\frac{n+3/2}{n+2}\right) + \log_2[2^B(n+1)]
\tag{49}
$$

results, which reduces to $B + \log_2(n)$ when the number of participating users is large. Therefore, multiuser selection policy based on SIR CQI provides a logarithmic increase in limiting achievable rate [10]. This is in contrast to previous findings, where system rate improvement due to multiuser diversity effect was only by a factor of a double logarithm with respect to the number of users.

5. Short-Term Fairness: Concepts and Performance Metric

Fairness in wireless networks indicates how equally radio resources are allocated among mobile users. Fairness should always be evaluated within a window in time. Those scheduling algorithms that obtain high fairness over a relatively short-time window are denoted as short-term fair, while the algorithms that obtain high fairness over an infinite-time window are denoted as asymptotically fair. The provision of short-term fairness characteristics for any multiuser diversity scheme is important because networking protocols usually have timers at different protocol layers that interact with each other in an unpredictable manner. An expiration of a timer is a bad event for an end-to-end connection. Such an event is usually interpreted as an indicator of congestion and loss of connectivity [22]. Thus, short-term fairness is always desirable for any packet scheduling procedures that reap multiuser diversity gain.

Several measures of fairness have been introduced in literature. Perhaps the simplest indicator is the so-called *Jain's fairness index* (JFI), introduced in [3] and used in recent papers such as [23] to characterize fairness behavior over a finite horizon:

$$
F_k(W) = \frac{\mathbb{E}_W^2\{R_k\}}{\mathbb{E}_W\{R_k^2\}} = \frac{\mathbb{E}_W^2\{R_k\}}{\mathbb{E}_W^2\{R_k\} + \text{Var}\{R_k\}},
\tag{50}
$$

where R_k is an RV that describes the amount of resource allocated to user k, $\mathbb{E}_W\{R_k\}$ is the expectation calculated within a time window of length W (time slots), and $\text{Var}\{R_k\}$ is the corresponding variance.

Jain's fairness index has several properties that makes it a suitable fairness measure. For example, the index is continuous and bounded between zero and unity. Moreover, JFI does not depend on the amount of the shared resource and on the number of participating users. The boundedness of JFI aids intuitive understanding of the fairness index. Even though an ideal fair distribution of common resources

would result in an index of 1, values above 0.95 are typically considered to indicate excellent fairness properties.

Resource allocation can be measured either in terms of the number of time slots assigned to a given user (within a window), or in terms of the throughput that was experienced by the user in these allocated time slots. However, here we only focus on the latter definition since achieving time-slot fairness in the presence of time-varying channels does not necessary imply a fair allocation of throughput in the assigned time slots. Throughput fairness curves for the different scheduling procedures introduced so far are presented in Section 6.3 with the goal of quantifying the short-term fairness performance that is sacrificed at the expense of obtaining additional multiuser diversity gain in our virtual MIMO system sum rate.

6. Performance Evaluation: Throughput-Fairness Behavior in Virtual MIMO

The actual virtual MIMO system sum rates for three different scheduling procedures and two CQI definitions are studied in this section based on intermediate results derived in Sections 3 and 4. The schedulers select at each time a pair of users that report orthogonal CDI codewords and differ with respect to their usage of CQI in scheduling decisions. Note that in those situations where scheduler fails to find a set of semiorthogonal users, the BS may either schedule transmission to a single user or resign the channel use at that time instant. Even though the former approach is most reasonable for a real-world system implementation, in this work we focus on the latter since we want to provide a representative characterization for TDMA and SDMA schemes when they work independently, leaving aside complex interactions between them that makes sum rate performance difficult to analyze.

6.1. Virtual MIMO System Sum Rate with CDI and No CQI. In this part, we consider the case of scheduling a pair of semiorthogonal users when no CQI is available at BS to perform user selection. We work on a simple case, known as pure ORR scheduler [12], where both primary and secondary users are selected in RR. Note that the performance in this case is equivalent to the one observed in case of PF scheduler when window size is tuned to optimize short-term fairness (large throughput tracking window). As expected, achievable sum rate is given by

$$C^{\mathrm{ORR}}(P) = 2C_k(P), \tag{51}$$

where closed-form approximation for $C_k(P)$ was derived in Section 3.3. Virtual MIMO system sum rate for pure ORR scheme is analyzed in Section 6.3. However, we now focus on analyzing the throughput behavior of an individual user when its selection does not take into account CQI reports.

Figure 1 shows the achievable rate (per beam) for pure ORR scheme when the CDI is represented by CL TD modes 1 and 2. The curves correspond to analytical approximation
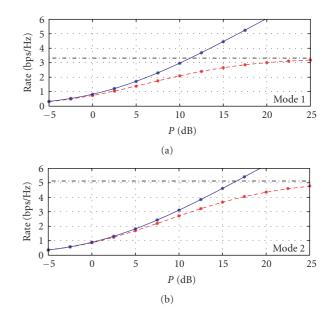

FIGURE 1: Achievable rate per beam for two-antenna mode 1 and 2 in the presence of Rayleigh fading and constant Tx power. Solid curves refer to TDMA-RR when total Tx power is normalized to $P/2$. Dashed curves refer to achievable rate per beam for spatial multiplexing with no CQI, and dash-dotted curves represent the asymptotic upper bound behavior presented in (22). In all cases, point values ("$*$") were simulated to verify the analytical results.

(51) (dashed curves) along with its corresponding asymptotic upper bounds (dash-dotted lines). The achievable rate for TDMA-RR is also included in these plots (solid lines). To make a fair comparison, Tx power in case of TDMA-RR is equal to the power per beam in case of pure ORR scheduling. As expected, the achievable rate for both TDMA-RR and pure ORR tends to be identical as Tx power decreases.

6.2. Virtual MIMO System Sum Rate with both CDI and CQI. Simple hybrid ORR proposals, known as ORR-Norm and ORR-SIR depending on the type of CQI that mobiles report, were introduced in [12] as improved versions of pure ORR scheme. These hybrid schedulers guarantee a certain degree of fairness by selecting the primary user according to its waiting time in transmission and exploit multiuser diversity in the selection of the secondary semiorthogonal user. Thus, achievable sum rate in this situation is now given by

$$
\begin{aligned}
C^{\mathrm{ORR}}_{\mathrm{CQI}}&(P, K) \\
&= C_k(P) \\
&+ \sum_{n=1}^{K-1} \left\{ \left[\binom{K-1}{n} (2^{-B})^n (1 - 2^{-B})^{K-n-1} \right] C^{\mathrm{CQI}}_{(n)}(P) \right\}.
\end{aligned}
\tag{52}
$$

The first term in (52) represents the achievable rate for the primary user selected in RR (Section 3.3), while the second term approximates the achievable rate for the secondary user
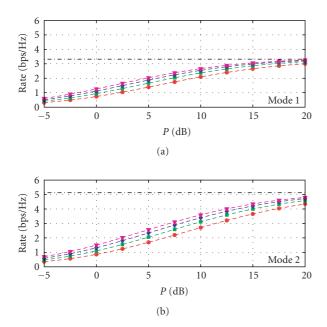
(a)

(b)

FIGURE 2: Achievable rate per beam for two-antenna mode 1 and 2 in the presence of Rayleigh fading and constant Tx power. Dashed curves refer to achievable rate per beam for spatial multiplexing with channel norm CQI and different number of users reporting identical CDI ($n = 1, 2, 4, 8$). Dash-dotted curves represent the asymptotic upper bound behavior presented in (22). In all cases, point values ("$*$") were simulated to verify the analytical results.
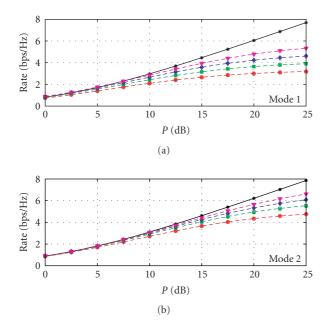

(a)

(b)

FIGURE 3: Achievable rate per beam for two-antenna mode 1 and 2 in the presence of Rayleigh fading and constant Tx power. Solid curves refer to TDMA-RR when total Tx power is normalized to $P/2$. Dashed curves refer to achievable rate per beam for spatial multiplexing with SIR CQI and different number of users reporting identical CDI ($n = 1, 2, 4, 8$). In all cases, point values ("$*$") were simulated to verify the analytical results.
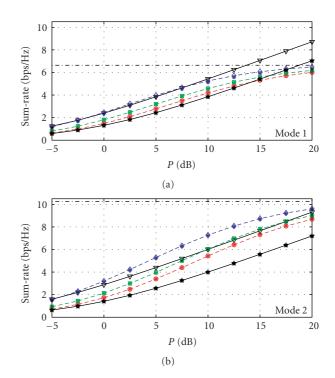

(a)

(b)

FIGURE 4: Virtual MIMO system sum-rate for two-antenna mode 1 ($K = 16$) and mode 2 ($K = 64$) in the presence of Rayleigh fading, constant Tx power, and channel norm CQI. Solid curves with stars ("$\star$") refer to TDMA-RR, while solid lines with triangles ("$\triangledown$") correspond to TDMA-BUS. Dashed curves with circles ("$\circ$"), dashed curves with squares ("$\square$") and dashed curves with diamonds ("$\diamond$") refer to pure ORR (ZFBF-PF throughput lower bound), ORR-Norm and ZFBF-SUS (ZFBF-PF throughput upper bound), respectively. Dash-dotted curves represent the asymptotic upper bound presented in (22). In all cases, point values ("$*$") were simulated to verify the analytical results.

selected according to the channel norm CQI (Section 4.2) and SIR CQI (Section 4.3).

Throughput upper bound for ZFBF-PF scheme is achieved when users instantaneous rates are not normalized by their average throughput before performing selection (small throughput tracking window). This is equivalent to choosing the set of users that maximize sum rate at each time slot without considering short-term fairness issues. It has already been observed in Section 2.2 that SUS procedure provides a simple way to obtain a set of semiorthogonal users with large CQI. Based on this, achievable sum rate in this situation can be represented by

$$C_{\text{CQI}}^{\text{SUS}}(P, K)$$

$$\lessapprox C_{(K)}^{\text{CQI}}(P)$$

$$+ \sum_{n=1}^{K-1} \left\{ \left[\binom{K-1}{n} (2^{-B})^n (1 - 2^{-B})^{K-n-1} \right] C_{(n)}^{\text{CQI}}(P) \right\}.$$

$$(53)$$

The first term in (53) represents the achievable rate of the user with the best CQI among all active users, while
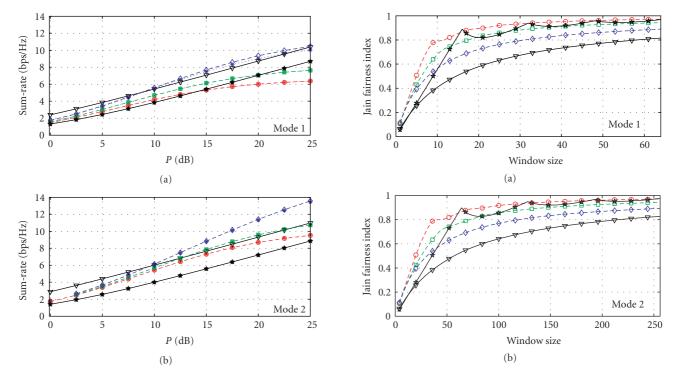
(a)

(b)

FIGURE 5: Virtual MIMO system sum-rate for two-antenna mode 1 ($K = 16$) and mode 2 ($K = 64$) in the presence of Rayleigh fading, constant Tx power, and SIR CQI. Solid curves with stars ("$\star$") refer to TDMA-RR, while solid lines with triangles ("$\triangledown$") correspond to TDMA-BUS. Dashed curves with circles ("$\circ$"), dashed curves with squares ("$\square$") and dashed curves with diamonds ("$\diamond$") refer to pure ORR (ZFBF-PF throughput lower bound), ORR-SIR and ZFBF-SUS (ZFBF-PF throughput upper bound), respectively. In all cases, point values ("$*$") were simulated to verify the analytical results.

FIGURE 6: Virtual MIMO system throughput fairness index for two-antenna mode 1 ($K = 16$) and mode 2 ($K = 64$) in the presence of Rayleigh fading, constant Tx power ($P = 5$ dB), and channel norm CQI. Solid curves with stars ("$\star$") refer to TDMA-RR, while solid lines with triangles ("$\triangledown$") correspond to TDMA-BUS. Dashed curves with circles ("$\circ$"), dashed curves with squares ("$\square$") and dashed curves with diamonds ("$\diamond$") refer to pure ORR (ZFBF-PF fairness upper bound), ORR-Norm and ZFBF-SUS (ZFBF-PF fairness lower bound), respectively.

the second term approximates the achievable rate of the user with the largest CQI among all users that satisfy orthogonality criterion (with respect to the first selected user). Note that final closed-form expression in this case is actually a tight upper bound because now independence assumption between ordered statistics of individual users rates in both terms is no longer valid. Virtual MIMO system sum rates for both hybrid ORR and ZFBF-SUS (both CQI definitions) are analyzed in Section 6.3. We now focus on the achievable rate of an individual user when its selection takes advantage of CQI reports.

Figures 2 and 3 show the achievable rate (per beam) when users are selected based on channel norms CQI and SIR CQI, respectively. These curves correspond to analytical approximations (29) and (42) (dashed curves), along with their simulated point values ("$*$"). Again, it is observed that the proposed approximations follow simulated values well for different numbers of users in both CL TD modes. As expected, the use of SIR CQI instead of channel norm CQI provides a better performance at high-SNR regimes.

6.3. Tradeoff Analysis of Throughput and Fairness in Virtual MIMO Systems. We are now ready to analyze the interaction

between overall system throughput and short-term throughput fairness that the different channel-aware scheduling procedures introduced so far are able to provide. In this context, Figures 4 and 5 present the actual virtual MIMO system sum rate for pure ORR, hybrid ORR-CQI, and ZFBF-SUS schemes when both channel norm CQI and SIR CQI are exploited, respectively. These curves correspond to analytical approximations (51), (52), and (53), along with their simulated point values ("$*$"). In addition, performances of TDMA-RR and TDMA-BUS (i.e., the TDMA scheme that selects the user with the highest channel gain at each time) are also included for the sake of comparison. To complement these plots, Figures 6 and 7 show the short-term fairness behavior for these schemes when using the fairness index introduced in (50) as a performance measure for different time-window horizons.

When analyzing these curves, it is straightforward to observe that, as expected, those schemes that reap higher multiuser diversity gain require a larger window size to achieve a certain degree of throughput fairness. Even though interesting tradeoffs between throughput and fairness can be reported when comparing these figures, perhaps the most important conclusion to highlight is that the simultaneous transmission to a set of smartly selected users provides
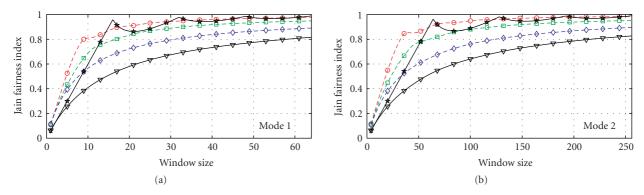
FIGURE 7: Virtual MIMO system throughput fairness index for two-antenna mode 1 ($K = 16$) and mode 2 ($K = 64$) in the presence of Rayleigh fading, constant Tx power ($P = 15$ dB), and SIR CQI. Solid curves with stars ("⋆") refer to TDMA-RR, while solid lines with triangles ("▽") correspond to TDMA-BUS. Dashed curves with circles ("∘"), dashed curves with squares ("□") and dashed curves with diamonds ("◇") refer to pure ORR (ZFBF-PF fairness upper bound), ORR-SIR and ZFBF-SUS (ZFBF-PF fairness lower bound), respectively.
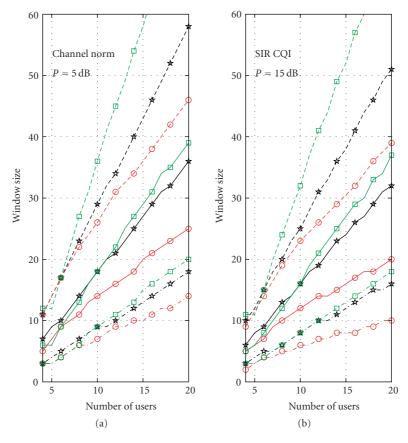

FIGURE 8: Required window size to achieve short-term throughput fairness with two-antenna mode 1 in the presence of Rayleigh fading, constant Tx power, and both CQI definitions. Curves with circles ("∘"), stars ("⋆") and squares ("□") refer to pure ORR, TDMA-RR and ORR-CQI, respectively. In all cases, dash-dotted curves represent a fairness index of 0.8, solid lines correspond to a fairness index of 0.9, and dashed curves refer to a fairness index of 0.95.

a better performance both, in terms of throughput and fairness, when compared to an analogous TDMA scheme. For example, when comparing TDMA-RR and pure ORR schemes, it is noticed that the latter provides as much as 15% (35%) more throughput in case of CL TD mode 1 (mode 2) without affecting considerably the short-term fairness degree that the former provides. Similar results

are obtained when comparing TDMA-BUS with ZFBF-SUS, but in this situation some throughput gain is traded off with an increase of the short-term fairness. It is important to highlight that the amount of CDI feedback does not impact considerably on the fairness of the schemes introduced so far if the ratio between the total number of users and the number of CDI codewords remains constant;

however, it actually has a direct effect on the multiuser diversity gain that these scheduling procedures provide , particularly when dealing with SIR CQI in high Tx power region.

Finally, Figure 8 shows the window size that is required to attain a certain level of short-term fairness as a function of the number of users in case of CL TD mode 1 with channel norm CQI ($P = 5$ dB) and SIR CQI ($P = 15$ dB), respectively. In these figures, dash-dotted curves represent a fairness index of 0.8, solid lines correspond to a fairness index of 0.9, and dashed curves refer to a fairness index of 0.95. Only TDMA-RR, pure ORR, and ORR-CQI schemes are included. This is because both ZFBF-SUS and TDMA-BUS do not provide acceptable fairness levels within practical window sizes. According to these curves, the time window that is required to achieve a certain degree of fairness grows linearly with the number of users. As expected, the slope of the curves depends not only on the requested fairness level, but also on the scheduling scheme. Note that both Tx power and CQI definition have a weaker effect on fairness performance. In all cases, pure ORR is the scheme with the best behavior. Note that the gap between TDMA-RR and ORR-CQI tends to grow as required level of fairness increases; however, for fairness levels up to 0.9, performance difference between these two schemes is almost negligible. We highlight that similar behavior is observed in case of CL TD mode 2.

7. Conclusions

In this paper, we investigated the tradeoff between maximizing system throughput and achieving throughput fairness in virtual MIMO downlink systems with quantized channel direction information and different types of channel quality information in the transmitter. We proposed a new theoretical approach to derive closed-form approximations to quantify throughput performance when combining different scheduling rules with zero-forcing beamforming. The short-term fairness analysis of the different schemes was performed using Jain's fairness index as performance metric. The advantages and disadvantages of the different schemes were highlighted by visualizing our closed-form expressions.

In our proposed theoretical model both desired signal energy and mutual interference in reception are modeled with first-order corrected versions of chi-square distributions, with characterization parameters obtained based on the first two raw statistics of these signals. The derived expressions were validated using existing 3GPP physical layer signaling structures. Our analysis revealed that simple scheduling procedures allow to reap a large fraction (in the order of 80%) of the sum-rate performance that greedy scheduling provides. This overall throughput performance was obtained without affecting considerably the optimal short-term fairness behavior that the end user would perceive.

Appendices

A. Error Correction

When approximating a generic distribution $f(\gamma)$ (with unknown closed-form formula) by a χ^2-distribution with r degrees of freedom and mean η, the error

$$\varepsilon(\gamma) = f(\gamma) - \frac{1}{\Gamma(r/2)}\left(\frac{r}{2\eta}\right)^{r/2}\gamma^{r/2-1}e^{-[r/(2\eta)]\gamma} \quad \text{(A.1)}$$

results. We shall express this error in terms of the raw moments $\mathbb{E}\{\gamma^n\}$ and the generalized Laguerre polynomials

$$L_k^{(\alpha)}(u) = \frac{u^{-\alpha}e^u}{k!}\frac{\partial^k}{\partial u^k}(e^{-u}u^{k+\alpha})$$

$$= \sum_{i=0}^{k}\binom{k+\alpha}{k-i}\frac{(-u)^i}{i!}. \quad \text{(A.2)}$$

These polynomials are orthogonal over the entire real line with respect to the weighting function $u^\alpha e^{-u}$; therefore,

$$\int_0^\infty u^\alpha e^{-u}L_k^{(\alpha)}(u)L_l^{(\alpha)}(u)du = \frac{(k+\alpha)!}{k!}\delta_{kl}, \quad \text{(A.3)}$$

where δ_{kl} is the Kronecker delta function. The orthogonality property stated above is equivalent to saying that if γ is a χ^2-distribution with r degrees of freedom and mean η, then

$$\mathbb{E}\{L_k^{(\alpha)}(\beta\gamma)L_l^{(\alpha)}(\beta\gamma)\} = \begin{cases} \dfrac{(k+\alpha)!}{\alpha!k!}, & k = l, \\ 0, & k \neq l \end{cases} \quad \text{(A.4)}$$

with $\alpha = r/2 - 1$ and $\beta = r/(2\eta)$. Hence, the error can be written as a series

$$\varepsilon(\gamma) = \frac{\beta}{\alpha!}(\beta\gamma)^\alpha e^{-\beta\gamma}\left[\sum_{k=2}^{+\infty}C_k^{(\alpha)}L_k^{(\alpha)}(\beta\gamma)\right]. \quad \text{(A.5)}$$

Series starts with $k = 2$ because moments of $\varepsilon(\gamma)$ of order up to 1 are null. In following sections, we show how can coefficients $C_k^{(\alpha)}$ be expressed in terms of the (known) raw moments of γ.

A.1. First-Order Correction for Exponential PDF Approximation. Let us first concentrate on the first-order error corrected version for $f(\gamma)$ when fading figure $\mathcal{F} \approx 1$. This approximation is obtained retaining the first nonzero term of the sum in (A.5), that is,

$$f(\gamma) \approx \frac{\beta}{\alpha!}(\beta\gamma)^\alpha e^{-\beta\gamma}[1 + C_2^{(\alpha)}L_2^{(\alpha)}(\beta\gamma)]. \quad \text{(A.6)}$$

Since in this case the exponential distribution (i.e., χ^2-distribution with $r = 2$ degrees of freedom) is the most suitable approximation, we have that $\alpha = 0$ and $\beta = 1/\eta$. It follows from (A.2) that

$$L_2^{(0)}(\beta\gamma) = \frac{1}{2}[(\beta\gamma)^2 - 4(\beta\gamma) + 2]. \quad \text{(A.7)}$$

Therefore, we only need to determine $C_2^{(0)}$. In order to do so, we have that

$$\int_0^\infty L_2^{(0)}(\beta\gamma)\varepsilon(\gamma)d\gamma$$

$$= \int_0^\infty L_2^{(0)}(\beta\gamma)\beta e^{-\beta\gamma}\sum_{k=2}^\infty [C_k^{(0)}L_k^{(0)}(\beta\gamma)]d\gamma$$

$$= C_2^{(0)}\int_0^\infty L_2^{(0)}(\beta\gamma)L_2^{(0)}(\beta\gamma)\beta e^{-\beta\gamma}\,d\gamma$$

$$+ \sum_{k=3}^\infty C_k^{(0)}\int_0^\infty L_2^{(0)}(\beta\gamma)L_k^{(0)}(\beta\gamma)\beta e^{-\beta\gamma}\,d\gamma. \qquad (A.8)$$

Orthogonality property introduced in (A.4) states that integral in the first term equals 1, while all integrals in the sum are null. Based on these considerations, it is possible to see that

$$\int_0^\infty L_2^{(0)}(\beta\gamma)\varepsilon(\gamma)d\gamma = C_2^{(0)}. \qquad (A.9)$$

Following an alternative analysis, that is, replacing $L_2^{(0)}(\beta\gamma)$ by expression (A.7), we also have that

$$\int_0^\infty L_2^{(0)}(\beta\gamma)\varepsilon(\gamma)d\gamma = \frac{1}{2}\int_0^\infty (\beta\gamma)^2\varepsilon(\gamma)d\gamma - 2\int_0^\infty (\beta\gamma)\varepsilon(\gamma)d\gamma$$

$$+ \int_0^\infty \varepsilon(\gamma)d\gamma. \qquad (A.10)$$

The last two integrals vanish because the moments of $\varepsilon(\gamma)$ of order up to 1 are null. Therefore,

$$\int_0^\infty L_2^{(0)}(\beta\gamma)\varepsilon(\gamma)d\gamma$$

$$= \frac{1}{2}\left[\int_0^\infty (\beta\gamma)^2 f(\gamma)d\gamma - \int_0^\infty (\beta\gamma)^2\beta e^{-\beta\gamma}\,d\gamma\right] \quad (A.11)$$

$$= \frac{\beta^2}{2}\left[\mathbb{E}\{\gamma^2\} - \frac{2}{\beta^2}\right].$$

Combining (A.9) and (A.11), $C_2^{(0)} = (1/2)\beta^2\mathbb{E}\{\gamma^2\}-1$ results. Replacing it in (A.6), final first-order corrected expression when fitting $f(\gamma)$ as an exponential RV with parameter $\beta^{-1} = \mathbb{E}\{\gamma\}$ results as follows:

$$f(\gamma) \approx \beta e^{-\beta\gamma}(a_2\gamma^2 + a_1\gamma + a_0),$$

$$a_2 = \frac{1}{4}\beta^4\mathbb{E}\{\gamma^2\} - \frac{1}{2}\beta^2, \ a_1 = -\beta^3\mathbb{E}\{\gamma^2\}+2\beta, \ a_0 = \frac{1}{2}\beta^2\mathbb{E}\{\gamma^2\}. \qquad (A.12)$$

A.2. First-Order Correction for χ^2-Distribution with Four Degrees of Freedom PDF Approximation. In this section, we work on the first-order error corrected version for $f(\gamma)$ when fading figure $\mathcal{F} \approx 2$. Again, this approximation is obtained retaining the first nonzero term of the sum in (A.5) considering $\alpha = 1$ and $\beta = 2/\eta$. Note that now the most

suitable χ^2-distribution to approximate $f(\gamma)$ should have $r = 4$ degrees of freedom. Therefore, approximation

$$f(\gamma) \approx \beta^2\gamma e^{-\beta\gamma}[1 + C_2^{(1)}L_2^{(1)}(\beta\gamma)] \qquad (A.13)$$

results. One more time, it is possible to derive from (A.2) that

$$L_2^{(1)}(\beta\gamma) = \frac{1}{2}[(\beta\gamma)^2 - 6(\beta\gamma) + 6]. \qquad (A.14)$$

Keeping in mind that we need to obtain $C_2^{(1)}$, it can be observed that

$$\int_0^\infty L_2^{(1)}(\beta\gamma)\varepsilon(\gamma)d\gamma$$

$$= \int_0^\infty L_2^{(1)}(\beta\gamma)\beta^2\gamma e^{-\beta\gamma}\sum_{k=2}^\infty [C_k^{(1)}L_k^{(1)}(\beta\gamma)]d\gamma$$

$$= C_2^{(1)}\int_0^\infty L_2^{(1)}(\beta\gamma)L_2^{(1)}(\beta\gamma)\beta^2\gamma e^{-\beta\gamma}d\gamma$$

$$+ \sum_{k=3}^\infty C_k^{(1)}\int_0^\infty L_2^{(1)}(\beta\gamma)L_k^{(1)}(\beta\gamma)\beta^2\gamma e^{-\beta\gamma}d\gamma. \qquad (A.15)$$

According to the orthogonality property introduced in (A.4), the integral in the first term is now equal to 3, while all the other integrals inside the sum remain null. Based on this, we find that

$$\int_0^\infty L_2^{(1)}(\beta\gamma)\varepsilon(\gamma)d\gamma = 3C_2^{(1)}. \qquad (A.16)$$

As an alternative approach, we now replace $L_2^{(1)}(\beta\gamma)$ by expression (A.14). Therefore,

$$\int_0^\infty L_2^{(1)}(\beta\gamma)\varepsilon(\gamma)d\gamma = \frac{1}{2}\int_0^\infty (\beta\gamma)^2\varepsilon(\gamma)d\gamma - 3\int_0^\infty (\beta\gamma)\varepsilon(\gamma)d\gamma$$

$$+ 3\int_0^\infty \varepsilon(\gamma)d\gamma. \qquad (A.17)$$

The last two integrals vanish because the moments of $\varepsilon(\gamma)$ of order up to 1 are null. Therefore,

$$\int_0^\infty L_2^{(1)}(\beta\gamma)\varepsilon(\gamma)d\gamma$$

$$= \frac{1}{2}\left[\int_0^\infty (\beta\gamma)^2 f(\gamma)d\gamma - \int_0^\infty (\beta\gamma)^2\beta^2\gamma e^{-\beta\gamma}\,d\gamma\right] \quad (A.18)$$

$$= \frac{\beta^2}{2}\left[\mathbb{E}\{\gamma^2\} - \frac{6}{\beta^2}\right].$$

Combining (A.16) and (A.18), we are able to arrive at $C_2^{(1)} = (1/6)\beta^2\mathbb{E}\{\gamma^2\} - 1$. Replacing this value in (A.13) allows us to conclude that the first-order error corrected version when

approximating $f(\gamma)$ with a χ^2-distribution with 4 degrees of freedom, and parameter $\beta^{-1} = (1/2)\mathbb{E}\{\gamma\}$ is equal to

$$f(\gamma) \approx \beta^2 \gamma e^{-\beta\gamma}(b_2\gamma^2 + b_1\gamma + b_0),$$

$$b_2 = \frac{1}{12}\beta^4 \mathbb{E}\{\gamma^2\} - \frac{1}{2}\beta^2,$$

$$b_1 = -\frac{1}{2}\beta^3 \mathbb{E}\{\gamma^2\} + 3\beta, \tag{A.19}$$

$$b_0 = \frac{1}{2}\beta^2 \mathbb{E}\{\gamma^2\} - 2.$$

B. SNR Gains and Fading Figures for W-CDMA Closed-Loop Transmit-Diversity Modes

Let us first compute the SNR gains when the best/worst Tx weight is selected for transmission. Working on (11) taking into account that $|w_{1,k}| = \sqrt{1 - \hat{\alpha}_k^2}$ and $|w_{2,k}| = \hat{\alpha}_k$,

$$\mathbb{E}\{X_k\} = (1 - \hat{\alpha}_k^2)\mathbb{E}\left\{|h_k|_{(2)}^2\right\} + \hat{\alpha}_k^2 \mathbb{E}\left\{|h_k|_{(1)}^2\right\}$$

$$+ 2\sqrt{1 - \hat{\alpha}_k^2}\,\hat{\alpha}_k \mathbb{E}\left\{|h_k|_{(1)}|h_k|_{(2)}\right\}\mathbb{E}\{\cos\varphi_k\},$$

$$\mathbb{E}\{Y_k\} = \hat{\alpha}_k^2 \mathbb{E}\left\{|h_k|_{(2)}^2\right\} + (1 - \hat{\alpha}_k^2)\mathbb{E}\left\{|h_k|_{(1)}^2\right\} \tag{B.1}$$

$$- 2\sqrt{1 - \hat{\alpha}_k^2}\,\hat{\alpha}_k \mathbb{E}\left\{|h_k|_{(1)}|h_k|_{(2)}\right\}\mathbb{E}\{\cos\varphi_k\}$$

result, where $|h_k|_{(1)}$ and $|h_k|_{(2)}$ are the first- and second-order statistic of two i.i.d. Rayleigh RVs with mean $\mathbb{E}\{|h_k|\} = \sqrt{\pi/4}$, respectively. Similarly, in case of second-order raw moments,

$$\mathbb{E}\{X_k^2\}$$

$$= (1 - \hat{\alpha}_k^2)^2 \mathbb{E}\left\{|h_k|_{(2)}^4\right\} + 2(1 - \hat{\alpha}_k^2)\hat{\alpha}_k^2 \mathbb{E}\left\{|h_k|_{(1)}^2|h_k|_{(2)}^2\right\}$$

$$\times \left[1 + 2\mathbb{E}\{\cos^2\varphi_k\}\right] + 4\sqrt{1 - \hat{\alpha}_k^2}\,\hat{\alpha}_k \mathbb{E}\{\cos\varphi_k\}$$

$$\times \left[(1 - \hat{\alpha}_k^2)\mathbb{E}\left\{|h_k|_{(1)}|h_k|_{(2)}^3\right\} + \hat{\alpha}_k^2 \mathbb{E}\left\{|h_k|_{(1)}^3|h_k|_{(2)}\right\}\right]$$

$$+ \hat{\alpha}_k^4 \mathbb{E}\left\{|h_k|_{(1)}^4\right\},$$

$$\mathbb{E}\{Y_k^2\}$$

$$= \hat{\alpha}_k^4 \mathbb{E}\left\{|h_k|_{(2)}^4\right\} + 2(1 - \hat{\alpha}_k^2)\hat{\alpha}_k^2 \mathbb{E}\left\{|h_k|_{(1)}^2|h_k|_{(2)}^2\right\}$$

$$\times \left[1 + 2\mathbb{E}\{\cos^2\varphi_k\}\right] - 4\sqrt{1 - \hat{\alpha}_k^2}\,\hat{\alpha}_k \mathbb{E}\{\cos\varphi_k\}$$

$$\times \left[\hat{\alpha}_k^2 \mathbb{E}\left\{|h_k|_{(1)}|h_k|_{(2)}^3\right\} + (1 - \hat{\alpha}_k^2)\mathbb{E}\left\{|h_k|_{(1)}^3|h_k|_{(2)}\right\}\right]$$

$$+ (1 - \hat{\alpha}_k^2)^2 \mathbb{E}\left\{|h_k|_{(1)}^4\right\} \tag{B.2}$$

result. In this situation, RV φ_k is uniformly distributed on $[-\pi/2^{N_p}, \pi/2^{N_p})$, where N_p is the number of bits used to quantize phase angles. Therefore, $\mathbb{E}\{\cos\varphi_k\} = (4/\pi)\sin(\pi/4)$ and $\mathbb{E}\{\cos^2\varphi_k\} = 1/2 + 1/\pi$ in case of CL TD mode 1, and

$\mathbb{E}\{\cos\varphi_k\} = (8/\pi)\sin(\pi/8)$ and $\mathbb{E}\{\cos^2\varphi_k\} = (1/2) + \sqrt{2}/\pi$ in case of CL TD mode 2. Similarly, $\hat{\alpha}_k = \sqrt{0.5}$ and $\hat{\alpha}_k = \sqrt{0.2}$ for both CL TD modes 1 and 2, respectively. Single raw moments and product raw moments of the order statistics of RV $|h_k|$ are obtained by using recurrence relations (13.4) and (13.7) of [24]. Replacing all these results, we find that

$$\mathcal{G}_x = 1 + \sqrt{\frac{1}{2}},$$

$$\mathcal{G}_y = 1 - \sqrt{\frac{1}{2}},$$

$$\mathbb{E}\{X_k^2\} = 2 + \frac{1}{\pi} + 3\sqrt{\frac{1}{2}}, \tag{B.3}$$

$$\mathbb{E}\{Y_k^2\} = 2 + \frac{1}{\pi} - 3\sqrt{\frac{1}{2}},$$

assuming CL TD mode 1, and

$$\mathcal{G}_x = 1.3 + 1.6\sin\left(\frac{\pi}{8}\right),$$

$$\mathcal{G}_y = 0.7 - 1.6\sin\left(\frac{\pi}{8}\right),$$

$$\mathbb{E}\{X_k^2\} = 2.9 + \left(4.8 + \frac{3.84}{\pi}\right)\sin\frac{\pi}{8} + \frac{1.28}{\pi}\sqrt{\frac{1}{2}}, \tag{B.4}$$

$$\mathbb{E}\{Y_k^2\} = 1.1 - \left(4.8 - \frac{3.84}{\pi}\right)\sin\frac{\pi}{8} + \frac{1.28}{\pi}\sqrt{\frac{1}{2}},$$

considering CL TD mode 2. Combining these raw moments in (8), fading figure expressions

$$\mathcal{F}_x = \frac{3/2 + 2\sqrt{1/2}}{1/2 + 1/\pi + \sqrt{1/2}}, \qquad \mathcal{F}_y = \frac{3/2 - 2\sqrt{1/2}}{1/2 + 1/\pi - \sqrt{1/2}}, \tag{B.5}$$

result assuming CL TD mode 1, and

$$\mathcal{F}_x$$

$$= \frac{2.97 + 4.16\sin(\pi/8) - 1.28\sqrt{1/2}}{-0.07 + 3.84(1/6 + 1/\pi)\sin(\pi/8) + 1.28(1 + 1/\pi)\sqrt{1/2}},$$

$$\mathcal{F}_y$$

$$= \frac{1.77 - 2.24\sin(\pi/8) - 1.28\sqrt{1/2}}{-0.67 + 3.84(-2/3 + 1/\pi)\sin(\pi/8) + 1.28(1 + 1/\pi)\sqrt{1/2}}, \tag{B.6}$$

considering CL TD mode 2.

C. Useful Closed-Form Expression

Our aim is to compute the integral

$$L_n(\beta, c) = \int_0^\infty \log_e(\gamma + c)\beta(\beta\gamma)^n e^{-\beta\gamma}\,d\gamma, \tag{C.1}$$

$$n = 0, 1, \ldots; \quad \beta > 0; \quad c > 0.$$

Let us use formula (8.356.4) of [25] and integrate (C.1) by parts. Then, we find that

$$L_n(\beta, c) = n! \log_e(c) + \int_0^\infty \frac{\Gamma(n+1, \beta\gamma)}{\gamma + c} d\gamma. \qquad \text{(C.2)}$$

Here, we have by (6.5.3), (6.5.2), (6.5.13), and (6.5.11) of [19] that

$$\int_0^\infty \frac{\Gamma(n+1, \beta\gamma)}{\gamma + c} d\gamma = n! \sum_{k=0}^n \frac{1}{k!} \int_0^\infty \frac{(\beta\gamma)^k e^{-\beta\gamma}}{\gamma + c} d\gamma. \qquad \text{(C.3)}$$

Then, by using (3.383.10) of [25] and (6.5.9) of [19], we obtain

$$\int_0^\infty \frac{(\beta\gamma)^k e^{-\beta\gamma}}{\gamma + c} d\gamma = k! e^{\beta c} E_{k+1}(\beta c). \qquad \text{(C.4)}$$

After combining the last three formulas, we get the desired result:

$$L_n(\beta, c) = n! \left[\log_e(c) + e^{\beta c} \sum_{k=0}^n E_{k+1}(\beta c) \right], \qquad \text{(C.5)}$$

$$n = 0, 1, \dots; \quad \beta > 0; \quad c > 0.$$

References

[1] R. W. Heath Jr., M. Airy, and A. J. Paulraj, "Multiuser diversity for MIMO wireless systems with linear receivers," in *Proceedings of the 35th Asilomar Conference on Signals, Systems and Computers*, vol. 2, pp. 1194–1199, Pacific Grove, Calif, USA, November 2001.

[2] P. Viswanath, D. N. C. Tse, and R. Laroia, "Opportunistic beamforming using dumb antennas," *IEEE Transactions on Information Theory*, vol. 48, no. 6, pp. 1277–1294, 2002.

[3] R. Jain, D. Chiu, and W. Hawe, "A quantitative measure of fairness and discrimination for resource allocation in shared computer systems," Tech. Rep. TR-301, Digital Equipment Corporation, Maynard, Mass, USA, September 1984.

[4] G. Caire and S. Shamai, "On the achievable throughput of a multiantenna Gaussian broadcast channel," *IEEE Transactions on Information Theory*, vol. 49, no. 7, pp. 1691–1706, 2003.

[5] H. Viswanathan, S. Venkatesan, and H. Huang, "Downlink capacity evaluation of cellular networks with known-interference cancellation," *IEEE Journal on Selected Areas in Communications*, vol. 21, no. 5, pp. 802–811, 2003.

[6] T. Yoo and A. Goldsmith, "On the optimality of multiantenna broadcast scheduling using zero-forcing beamforming," *IEEE Journal on Selected Areas in Communications*, vol. 24, no. 3, pp. 528–541, 2006.

[7] A. Narula, M. J. Lopez, M. D. Trott, and G. W. Wornell, "Efficient use of side information in multiple-antenna data transmission over fading channels," *IEEE Journal on Selected Areas in Communications*, vol. 16, no. 8, pp. 1423–1436, 1998.

[8] D. J. Love, R. W. Heath Jr., and T. Strohmer, "Grassmannian beamforming for multiple-input multiple-output wireless systems," *IEEE Transactions on Information Theory*, vol. 49, no. 10, pp. 2735–2747, 2003.

[9] K. K. Mukkavilli, A. Sabharwal, E. Erkip, and B. Aazhang, "On beamforming with finite rate feedback in multiple-antenna systems," *IEEE Transactions on Information Theory*, vol. 49, no. 10, pp. 2562–2579, 2003.

[10] T. Yoo, N. Jindal, and A. Goldsmith, "Multi-antenna downlink channels with limited feedback and user selection," *IEEE Journal on Selected Areas in Communications*, vol. 25, no. 7, pp. 1478–1491, 2007.

[11] 3GPP, "Physical layer procedures (FDD)," Technical Specification TS 25.214, V5.6.0, 3GPP, Valbonne, France, 2003.

[12] A. A. Dowhuszko, G. Corral-Briones, J. Hämäläinen, and R. Wichman, "Achievable sum-rate analysis of practical multiuser scheduling schemes with limited feedback," in *Proceedings of IEEE International Conference on Communications (ICC '07)*, pp. 4381–4386, Glasgow, Scotland, June 2007.

[13] 3GPP, "Physical layer aspects of UTRA high speed downlink packet access," Tech. Rep. TSG-RAN TR 25.858 V 5.0.0, 3GPP, Valbonne, France, 2002.

[14] R. J. McEliece and W. E. Stark, "Channels with block interference," *IEEE Transactions on Information Theory*, vol. 30, no. 1, pp. 44–53, 1984.

[15] S. Sanayei and A. Nosratinia, "Opportunistic beamforming with limited feedback," *IEEE Transactions on Wireless Communications*, vol. 6, no. 8, pp. 2765–2771, 2007.

[16] J. Diaz, O. Simeone, and Y. Bar-Ness, "Sum-rate of MIMO broadcast channels with one bit feedback," in *Proceedings of IEEE International Symposium on Information Theory (ISIT '06)*, pp. 1944–1948, Seattle, Wash, USA, July 2006.

[17] A. Jalali, R. Padovani, and R. Pankaj, "Data throughput of CDMA-HDR a high efficiency-high data rate personal communication wireless system," in *Proceedings of the 51st IEEE Vehicular Technology Conference (VTC '00)*, vol. 3, pp. 1854–1858, Tokyo, Japan, May 2000.

[18] M. Nakagami, "The m-distribution—a general formula for intensity distribution of rapid fading," in *Statistical Methods in Radio Wave Propagation*, pp. 581–635, McGraw-Hill, New York, NY, USA, 1958.

[19] M. Abramowitz and I. A. Stegun, *Handbook of Mathematical Functions*, National Bureau of Standards, Washington, DC, USA, 1970.

[20] A. A. Dowhuszko, G. Corral-Briones, J. Hämäläinen, and R. Wichman, "Outage probability analysis of practical multiuser scheduling schemes with limited feedback," in *Proceedings of the 65th IEEE Vehicular Technology Conference (VTC '07)*, pp. 1036–1040, Dublin, Ireland, April 2007.

[21] S. Zhou, Z. Wang, and G. B. Giannakis, "Quantifying the power loss when transmit beamforming relies on finite-rate feedback," *IEEE Transactions on Wireless Communications*, vol. 4, no. 4, pp. 1948–1957, 2005.

[22] S. S. Kulkarni and C. Rosenberg, "Opportunistic scheduling policies for wireless systems with short term fairness constraints," in *Proceedings of IEEE Global Telecommunications Conference (GLOBECOM '03)*, vol. 1, pp. 533–537, San Francisco, Calif, USA, December 2003.

[23] V. Hassel, M. R. Hanssen, and G. E. Øien, "Spectral efficiency and fairness for opportunistic round robin scheduling," in *Proceedings of IEEE International Conference on Communications (ICC '06)*, vol. 2, pp. 784–789, Istanbul, Turkey, June 2006.

[24] N. Balakrishnan and C. Rao, Eds., *Handbook of Statistics 16: Order Statistics: Theory & Methods*, Elsevier, Amsterdam, The Netherlands, 1998.

[25] I. Gradshteyn and I. Ryzhik, *Table of Integrals, Series, and Products*, Academic Press, New York, NY, USA, 2007.